Relationship between morphology and electrical properties in PP/MWCNT composites: Processing-induced anisotropic percolation threshold

UNIVERSITÀ DEGLI STUDI DI TORINO

Materials Chemistry and Physics (Elsevier)
Volume 180, 1 September 2016, Pages 284-290
DOI: 10.1016/j.matchemphys.2016.06.009

Relationship between morphology and electrical properties in PP/ MWCNT composites: Processing-induced anisotropic percolation threshold

F. Cesano [a, *], M. Zaccone [b, c], I. Armentano [d], S. Cravanzola [a], L. Muscuso [a], L. Torre [d], J.M. Kenny [c, d], M. Monti [b], D. Scarano [a]

[a] *Department of Chemistry, NIS (Nanostructured Interfaces and Surfaces) Interdepartmental Centre and INSTM Centro di Riferimento, University of Torino, Via P. Giuria, 7, 10125 Torino, Italy*

[b] *Proplast, Strada Comunale Savonesa 9, 15057 Rivalta Scrivia, AL, Italy*

[c] *ECNP, Strada Comunale Savonesa 9, 15057 Rivalta Scrivia, AL, Italy*

[d] *Materials Engineering Center, UdR INSTM, University of Perugia, Str. Pentima 4, 05100 Terni, Italy*

* Corresponding author. E-mail address: federico.cesano@unito.it (F. Cesano).

A b s t r a c t

Multi-walled carbon nanotubes (MWCNTs)/polypropylene composites were prepared by melt-mixing, by varying the MWCNT content from 1 to 7 wt%, and samples were manufactured by injection moulding technique.

DC electrical characterization was performed by the two-probe method in the three main directions: longitudinal and transversal to the flux of the material during the mould filling, and in the through-thickness direction. Moreover, a dedicated setup was adopted to measure the electrical resistance at different depths of the specimen cross-sectional areas. Two different electrical percolation thresholds, calculated at about 2 wt% and 3 wt% of MWCNTs (longitudinally/transversely to the mould filling flux and in the through-thickness directions, respectively), were found. In order to investigate the role of the structure/morphology of the composites on the electrical properties, samples have been cryofractured, chemically etched and characterized by means of scanning electron microscopy. As a result, the observed anisotropic electrical behaviour was associated with the different network morphology, which was detected in the cross-sectional area, caused by the injection moulding process. Based on the observed through-thickness electrical behaviour, a phenomenological DC conduction model has been developed, describing the sample as a multilayer system, being the external layers (skin) less conductive than the internal region (core). This model, combined with the bulk electrical tests, can be considered as a valuable mathematical tool to foresee the electrical behaviour of MWCNT-based composites for designing new industrial injection-moulded components.

1. Introduction

In the last decades, the interest in polymers with conductive properties, coming from the combination with electrically active nanomaterials, has increased considerably [1]. In fact, new opportunities and applications come from the union of the peculiar properties of a polymer, such as simplicity of manufacturing, lightweight, resistance to chemical corrosion, and the peculiar mechanical and electrical properties of the conducting fillers [2,3]. Among the carbon-based nanomaterials with different shape and aspect ratio [4,5], multi-walled carbon nanotubes (MWCNTs) have attracted considerable attention and are identified as one of the most promising nanostructures to obtain multifunctional materials for industrial applications [6,7], including devices for sensor technology [8e10], thermally conductive components [11e13], electrical conducting and/or electromagnetic interference-shielding systems [14e19]. In particular, it was hypothesized that carbon nanotubes can carry an electrical current density up to $z10^9e10^{10}$ A/cm^2 [20], which is more than 1000 times greater than metals. Moreover, since their first discovery by Iijima at the beginning of 90s [21], CNTs have reached a technological maturity and a cost-to-performance ratio, which is suitable for a real market exploitation.

Carbon nanotubes, with their high aspect ratio and chain-like aggregate structures, have a greater tendency to form a conductive network within the polymer matrix, if compared with other conductive additives [22]. It comes out that the electrical properties of the carbon-based polymer composites are due to the transport of the electrons, guaranteed by a conductive network of continuous contacts, thus creating a pathway for the transfer of electrons within the polymer matrix, according to the percolation theory [22e25].

Many factors can affect the conductivity of the polymer composites, such as the polymer type, content of the conducting carbon fillers and the type (in terms of shape, aspect ratio and morphological characteristics), the surface properties of the fillers, the nature of the polymer and finally the processing conditions [1,3,26]. As for the extrusion processing conditions, it has been observed that, by increasing the screw speed, the conductivity is decreasing because of the presence of a segregated structure of carbon nanofillers, within the compacted polymer phase [27]. Moreover, it is reported that a skin-core morphology of injection-moulded pure polymer (i.e. PP with a different molecular weight distribution and crystallinity) [28] or CNT-based polymer composites [29,30], can be obtained. In the specific case of CNT/polymer composites, the orientation of nanotubes, induced by the shear rate nearby the surface, may be larger than that in the body, as well as the different local concentrations of CNT in the skin layer and in the core region [31]. The peculiar skin-core microstructure may be of interest for several applications, including the integrated monitoring and sensing based on smart components [8,9,30]. From all these considerations, it is clear that the carbon nanotube dispersion is the key point in determining the conductivity performances of the composite [32e36]. In particular, in most of the techniques for obtaining final plastic items, the morphology of CNT-polymer composites is strongly influenced by the shaping phase, when the polymer is in the molten state. As an example, in the injection moulding and extrusion techniques e as far as the thermoplastic matrices are concerned e it is widely known that the longitudinal flux of the molten polymer can induce an alignment in micro-sized fibers, (e.g. carbon and glass fibers) [37], and in nano-sized particles [35].

In this paper, polypropylene (PP) composites filled with MWCNTs were developed. The MWCNT dispersion was performed in a co-rotating twin-screw extruder, and the obtained composites were injection moulded.

Electrical characterization was then performed in the three main directions, that are: i) longitudinal to the flux of the material during the mould filling, ii) transversal to the flux and iii) the through-thickness direction. The effect of processing on the anisotropic electrical percolation threshold (P_c), defined as the insulator-to-conductor transition and the associated MWCNT network morphology was deeply investigated and analyzed also by a phenomenological conduction model. Interestingly, the obtained results may provide a robust platform to gain insight into polymer-carbon nanotube dispersion, being an important step in the study and control of the morphology/electrical properties of the MWCNT composites.

2. Experimental

2.1. Materials

Multi-walled carbon nanotubes (Nanocyl NC7000) were used as fillers. As reported by the manufacturer, they are 10e20 nm in diameter and 1.5e2 mm in length. Polypropylene (PP) Moplen RP 348 R (Lyondell Basell) was selected as a polymer matrix. It is a random copolymer (injection moulding grade), with a MFI of 25 g/10 min (230 °Ce2.16 kg) and a density of 900 kg/m^3. Several contents of MWCNTs were added to the PP, namely 1-2-3-4-5-6-7 wt%.

MWCNTs were homogeneously mixed with the polymer by melt compounding technique in a corotating twin-screw extruder (Leistritz 27E). This extruder has a screw diameter D of 27 mm and a length of 40D, and it can be considered a pilot line, which well simulates the industrial process of thermoplastic polymer compounding. Polymer was fed through a Brabender metering unit at the beginning of the extrusion line through the main feeder, while MWCNTs were fed through the side feeder, which is placed at two-third of the screw length from the extrusion die. The processing temperatures were set as shown in Fig. 1a.

The obtained composite mixtures were used to produce square-shaped samples (100 x 140 x 2.25 mm in size) by injection moulding technique, using a Ferromatik 110 press, with the processing temperatures reported in Fig. 1b. The used mould was designed specifically for minimizing the rupture of MWCNTs during the filling process and characterized by a fan gate (see Fig. 1c), which can uniform the flux of the molten material while filling the mould. The design and the 3D Cartesian coordinate system (X, Y, Z axes) of the sample is also reported in Fig. 1c.

2.2. Methods

DC electrical characterization was performed by the two-probe

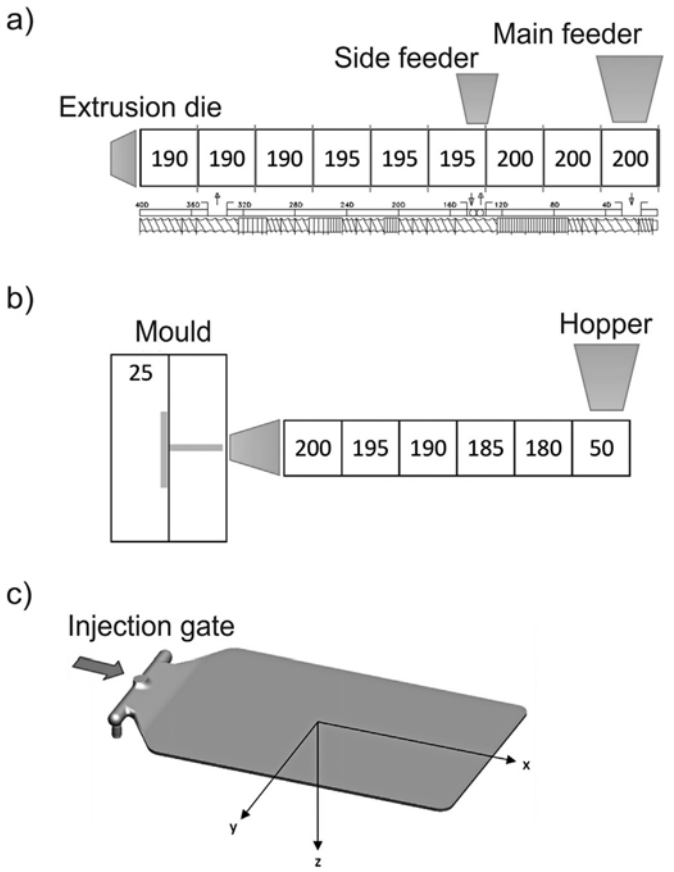

Fig. 1. a) Extrusion and injection moulding scheme b) processing temperatures and layout, c) scheme of the sample produced by injection moulding. The injection point/ flow directions are shown by the arrow.

method by means of the r ¼ R A/D equation (where R is the resistance in Ohm, A is the cross-sectional area in cm^2 and D is the distance between the two electrodes in cm). Low-resistance wiring and connections were verified before sample analysis. Resistivities of samples (Ohm cm) were consequently obtained in the three main directions: i) longitudinal to the flux (X) of the material during the mould filling, ii) transversal to the flux (Y) and iii) in the through-thickness direction (Z). The test setup adopted for the electrical measurements along the different directions are reported in Fig. 2a and b.

In order to ensure high-accuracy high-resistance measurements, the electrical properties along the Z direction electrical resistivity measurements were conducted by using a Keithley 6517B electrometer (electrode dimensions: 20.971 cm^2) combined with a Keithley 8009 test fixture, which guarantees the good electrostatic shielding and high insulation resistance.

In order to measure the electrical properties along X and Y, the specimens were cut (20 x 2.25 x 4 mm) from the injection moulded samples. A silver-based conductive paste was used to obtain two ohmic contacts with a good low-resistance (A, 0.225 x 0.4 cm), 0.3 cm spaced (D) on the obtained specimens. The current (I) was measured by the two-probe method with a digital multimeter (Keithley 2420) by applying a potential in the 1 ÷ 20 V range, and the corresponding resistance (R) was obtained.

A dedicated setup was developed and adopted to measure the influence of the Z-coordinate in the electrical properties of a cross sectional area. Tests were performed using a Keithley 2420, by means of two m-electrodes (both perpendicular to Z), which are placed in contact with the specimen at intervals of 250 mm along the whole sample thickness, from the top to the bottom surface, as shown in Fig. 2c. More in detail, the two Tungsten Carbide electrodes (100 mm in diameter) were separated by a distance of 1000 ± 10mm and moved by means of a micrometer screw-driven XY-axes platform. Each of the electrodes in the back side is connected to a spring under a low loading (30 g) to prevent damage on the sample during the measurement. The spatial resolution during the measurements was estimated to be as low as 200 mm.

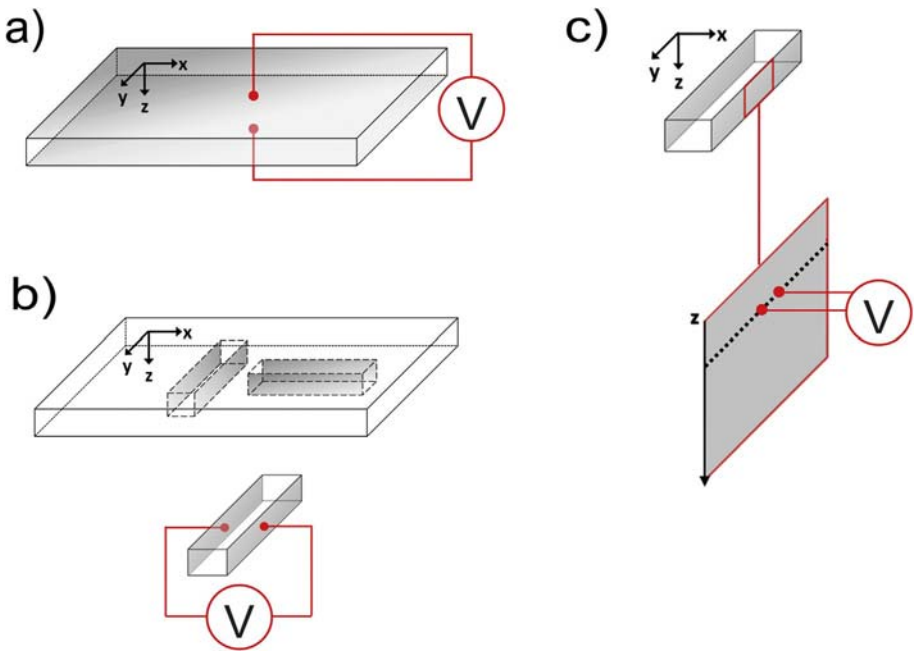

Fig. 2. Experimental setup of DC electrical measurements: tests in the a) Z-direction; b) X- and -Y- directions; c) the setup developed to measure the influence of the Z-coordinate in the electrical properties of the cross sectional area of the sample.

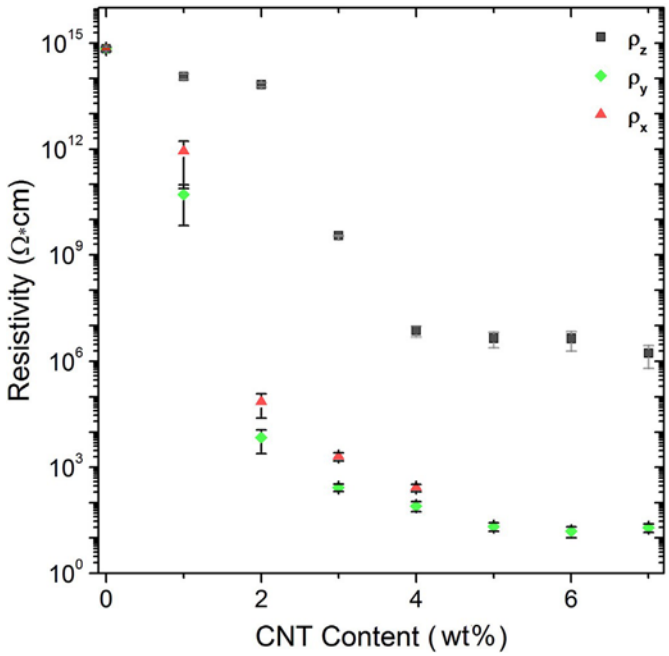

Fig. 3. DC resistivity versus MWCNT content in polypropylene: Z- (black squares) Y- (green rhombus) and X-directions (red triangles), respectively. (For interpretation of the references to colour in this figure legend, the reader is referred to the web version of this article.)

The morphology of the samples has been investigated by means of a Zeiss Evo50 SEM instrument. Samples were preventively cryo-fractured and chemically etched for 15 h [9].

3. Results and discussion

3.1. Electrical properties and morphology

Electrical resistivities of the MWCNT/PP composites as a function of the MWCNT content along the three main directions are shown in Fig. 3.

According to the obtained results, several remarks can be made. First of all, after the conversion to conductivity values (S), the obtained percolation threshold values (about 2 wt% and about 3 wt% along X-Y and Z directions, respectively) (Supplementary Data), are to some extent higher than those described in some papers [15,19], but quite similar to those reported for the semi-industrial scale production of injection-moulded MWCNT-based PP and PE composites [9,38]. Furthermore, by comparing the curves related to the X and Y directions (Fig. 3), no significant differences can be observed, testifying that no CNT orientation along the flux direction (X) has been produced during the injection moulding process, in agreement with what is expected for medium viscosity melts ($h_0 \geq 10^2 e 10^3$ Pa$s) obtained under a medium or low apparent shear rates [27,39].

This is further demonstrated by the morphological analysis performed by SEM. As an example, Fig. 4 shows the fracture surfaces of the 3 wt% MWCNT composite, perpendicular to the X and Y direction respectively. From this figures it can be observed that, in both cases MWCNTs form disordered entanglements with no preferential direction, and no significant difference can be detected from one section to the other.

The most interesting outcome shown in Fig. 3 is related to the comparison of the P_c in the Z direction, which is different from the one of X and Y direction. In fact, the electrical percolation threshold is in the range of 3 wt% for the Z direction and 1e2 wt% for the X and Y direction. Moreover, the electrical resistivity reaches a different plateau value in the Z direction with respect to X and Y ones, being about 10^1 U cm (along the X and Y directions) and 10^6 Ucm (along the Z-direction). It is worthy noticing that for measurements along the Z direction the two electrodes are both contacting the specimen surface, while for measurements along X and Y directions new exposed surfaces, before belonging to the bulk region, are measured.

In order to understand the difference in the electrical properties in the three main directions, a thorough study on the influence of the z-coordinate in the electrical properties of the cross sectional area was performed with the 2-3-4 wt% MWCNT-based samples. These contents were chosen because they are in the range of the electrical percolation threshold.

Fig. 5 shows the results of the surface electrical resistance as a function of the depth. The top and bottom of the graph (ordinate axis) represents the two external sides of the injection moulded sample. Note that some values are missing due to the electrical resistance higher than the detectable limit of the used equipment. From this figure, it can be inferred that the electrical resistance is not constant in the sample thickness, being higher moving towards the external regions. In particular, this variation is smaller for the lower MWCNT contents, where for the 2 wt% it increases from the order of 10^6 U in the internal region (core) to 10^7 U in the external layers (skin), and for the 3 wt% from the order of 10^5 U in the internal region to 10^7 U in the external layers. In the case of 4 wt% the electrical resistance varies from 10^5 U in the internal region to 10^7 U in the external layers. However, it deserves to be underlined that in the 4 wt% MWCNT composite, the internal more-conductive region is wider than in the other studied composites, and the conductivity in this region is nearly constant at about 2×10^5 U. From the graph, the thickness of the external less-conductive layers can be roughly estimated to be about 250 mm, with a resulting thickness of the more-conductive region of about 2 mm. In the case of 2 and 3 wt%

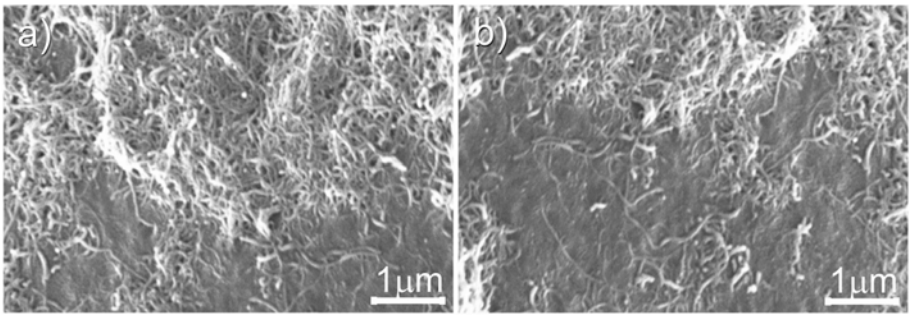

Fig. 4. SEM images of the MWCNT polymer composite (MWCNTs ¼ 3 wt%), as obtained along the x-a) and the y-b) axis directions.

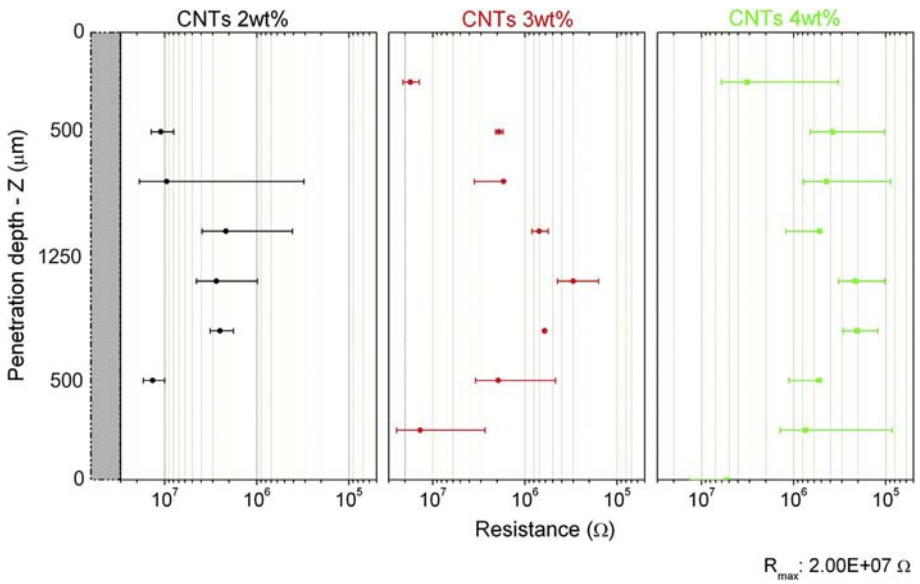

Fig. 5. Two-probe surface resistance versus penetration depth for: 2 wt% (black points, left panel), 3 wt% (red points, middle panel), 4 wt% (green points, right panel) MWCNTsePP composites, respectively. (For interpretation of the references to colour in this figure legend, the reader is referred to the web version of this article.)

MWCNT composites, the electrical resistance in the internal region is not constant and seems to have a parabolic-like trend, with the maximum in the middle. In these cases, the thickness of the external less-conductive layers can be roughly estimated to be about 500 mm, with a resulting thickness of the more-conductive region of about 1.25 mm.

In order to explain the obtained results, an in-depth morphological characterization was performed by scanning electron microscopy (SEM). Fig. 6 reports SEM images of 2, 3 and 4 wt%, obtained both in the external layer (Fig. 6a,c,e) and in the internal region (Fig. 6b,d,f), respectively. The 2 wt% MWCNT composite morphology is based on filler-rich areas with agglomerates well

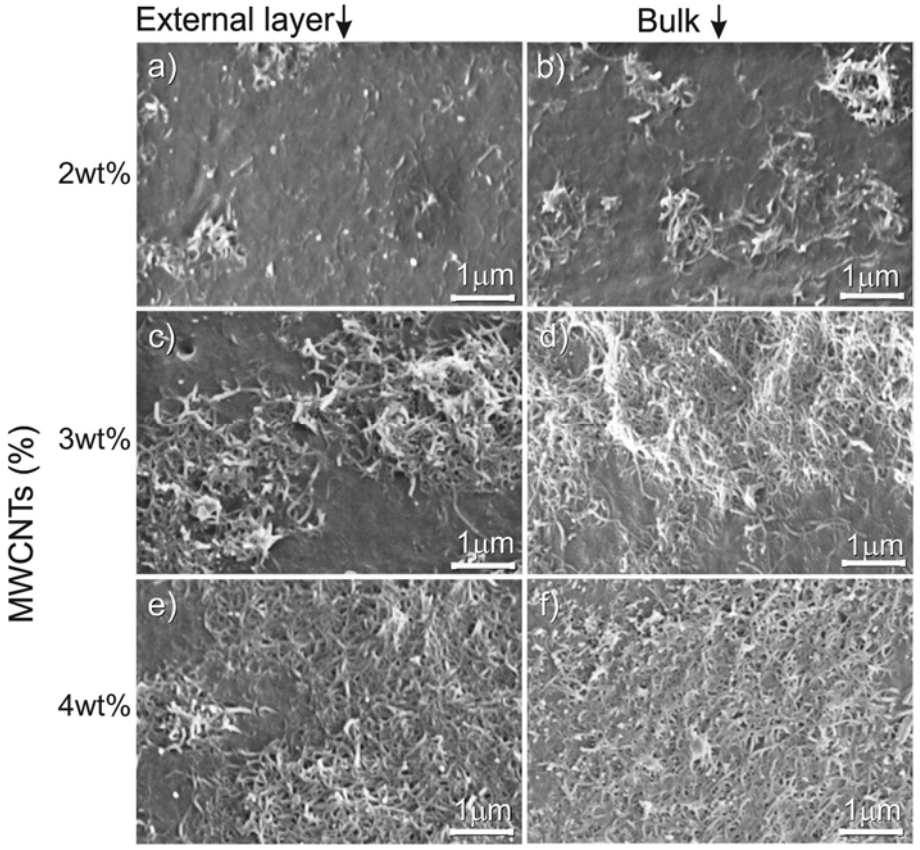

Fig. 6. Cross-section SEM images of MWCNT-based PP composites (2 wt%, 3 wt% and 4 wt% MWCNTs) obtained in the external (a, c, e) and in the core regions (b, d, f), respectively.

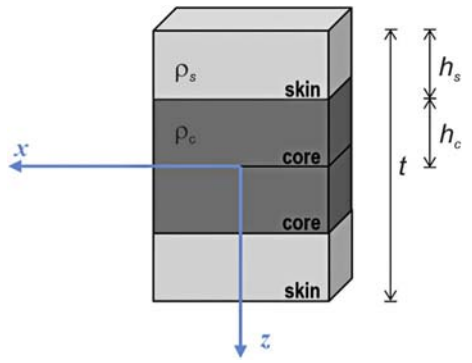

Fig. 7. Scheme of the injection moulded samples, described as four layers stacked in the thickness direction.

impregnated by the polymer matrix, interconnected by resin-rich areas. The 3 and 4 wt% MWCNT composite are characterized by a homogeneous distribution of MWCNT agglomerates well impregnated by the polymer matrix. In all cases, the internal region seems to be richer of MWCNTs than the external layer. In particular, this is more evident in the case of the lower contents, while for the 4 wt% the difference is faded, although still detectable. The formation of a conductive filler network, occurring at higher filler content and to a greater extent in the core regions, (clustering or secondary agglomeration state), leads to conductive paths, which can explain the before-discussed electrical properties [27]. As a consequence, it is possible to conclude that the skin layer covering the external region of the compounds is characterized by a lower conductivity, while the core region already becomes conductive at lower filler content.

3.2. Electrical behaviour: the proposed model

The results of the electrical characterization (Figs. 3 and 5) can be exploited to develop a scheme for modelling the through-thickness electrical behaviour of injection-moulded components. Based on experimental outcomes, the injection-moulded samples can be modelled as a multilayer system, being the external layers (the skin) less conductive and the internal region (the core) more conductive, due to the different distribution of the MWCNTs in the two parts, as confirmed by SEM images (Fig. 6). From this model, the overall resistivity is affected by the electrical properties of the skin and of the core regions, as well as by their relative sizes.

The proposed model is based on four layers stacked in the through-thickness direction, each one with its own electrical resistivity, symmetric with respect to the mid-plane (see Fig. 7).

According to this model based on parallel-series resistors, the Z-direction overall electrical resistance (R) should be governed by resistor series corresponding to the 4 layers, while the X-direction electrical resistance is taken parallel to the same system. The following system can be written substituting the well-known equation $R = \rho l/A$, where l and A are the length of the resistor and the surface of the electrode, respectively:

$$\begin{cases} \rho_x = 2\dfrac{\rho_s \rho_c}{\rho_s h_c + \rho_c h_s} \\ \rho_z t = 2(\rho_s h_s + \rho_c h_c) \end{cases} \tag{1}$$

where ρ_x and ρ_z are the electrical resistivities calculated experimentally (and reported in Fig. 3) and t is the thickness of the sample ($t = 2.25$ mm). Subscripts s and c refer to the skin and the core layer, respectively, as hypothesized by the proposed model; in particular, ρ_s and ρ_c are the electrical resistivity, and h_s and h_c are the thicknesses of the skin layer and the core layer, respectively.

The thickness of the two layers has been approximately evaluated by the results reported in Fig. 5. Indeed, a threshold can be detected between the non-conductive or nearly non-conductive area at the edges and the more conductive area in the inner part of the section. The threshold can be used to identify the skin and the core layers defined in the proposed model. The thickness values (h_s and h_c) estimated from Fig. 5 for the 2, 3, 4 wt% MWCNT composites are reported in Table 1.

The system (1) can be easily solved to calculate ρ_s and ρ_c, taking into account only the solution with a physical meaning:

$$\begin{cases} \rho_s = \dfrac{-\rho_x h_c + \rho_x h_s + \rho_z t + \sqrt{(\rho_x h_c - \rho_x h_s - \rho_z t)^2 - 4\rho_x \rho_z h_s t}}{4 t h_s} \\ \rho_c = \dfrac{\rho_z t - 2\rho_s h_s}{2 h_c} \end{cases} \tag{2}$$

The results of the system have been calculated for the three MWCNT contents and compared to the measured resistivity in the Z and X direction (Table 1).

The proposed model allows one to thoroughly understand the electrical behaviour of an injection-moulded component, taking into account the skin-core character, which is induced by the flow of the molten material inside the mould, during manufacturing. Furthermore, the obtained anisotropic conductivity can be correlated to the dynamic flux of the molten polymer inside the mould, which is inducing the formation of a poorly conductive external layer.

4. Conclusions

MWCNTs have been successfully mixed with polypropylene through a melt mixing process in a co-rotating twin-screw extruder, and samples have been manufactured by injection moulding technique.

The electrical characterization of the produced composites has shown that the electrical behaviour is different when the tests are performed along the three main directions. In fact, the electrical percolation threshold and the plateau value of the electrical resistivity are higher for the through-thickness direction, while these parameters do not vary significantly along the in-plane directions.

Table 1
Results of the proposed model as a function of the MWCNT content.

MWCNT content [wt%]	Input				Output	
	ρ_z [Ohm cm]	ρ_x [Ohm cm]	h_s [cm]	h_c [cm]	ρ_s [Ohm cm]	ρ_c [Ohm cm]
2	6.65E+13	1.17E+05	5.00E-02	6.25E-02	1.50E+14	1.62E+04
3	3.49E+09	1.92E+03	2.50E-02	8.75E-02	1.57E+10	3.73E+02
4	4.82E+06	2.85E+02	2.50E-02	8.75E-02	2.17E+07	5.53E+01

Moreover, the electrical resistance in the cross-sectional area has been evaluated at different depths. From these tests, it was shown that the electrical resistance increases when moving from the internal area toward the external skin. This change is caused by the different morphology of the cross sectional area. More in detail, in the internal region a processing-induced higher density of MWCNTs was observed, if compared with the external layers.

In conclusion, the injection moulding process induces an inhomogeneous distribution of the MWCNTs in the cross sectional area, which influences the electrical behaviour of the injection moulded component. This behaviour can be predicted and mathematically schematized by the simple phenomenological model proposed in this study. The advanced design of an electrically conductive injection moulded component can lead to an optimization of the final performance. Therefore, the obtained results may provide a robust platform to gain insight into polymer-carbon nanotube dispersion, being an important step in the study and control of the morphology and of the electrical properties of the MWCNT composites.

Acknowledgments

The research was supported from the funding of Regione Piemente (Italy) (POR FESR 2007/2013, Linea di attivita' I.1.1. "Piattaforme innovative" - Bando Automotive), under the Drapo Project. This work was also supported by MIUR (Ministero dell'Istruzione, dell'Universita e della Ricerca), INSTM Consorzio and NIS (Nanostructured Interfaces and Surfaces) Inter-Departmental Centre of University of Torino.

Appendix A. Supplementary data

References

[1] G. Mittal, V. Dhand, K.Y. Rhee, et al., A review on carbon nanotubes and graphene as fillers in reinforced polymer nanocomposites, J. Ind. Eng. Chem. 21 (2015) 11e25.
[2] Z. Liu, Y. Song, Y. Shangguan, et al., Conductive behavior of composites composed of carbon black-filled ethylene-tetrafluoroethylene copolymer, J. Mater. Sci. 42 (2007) 2903e2906.
[3] G. Haznedar, S. Cravanzola, M. Zanetti, et al., Graphite nanoplatelets and carbon nanotubes based polyethylene composites: electrical conductivity and morphology, Mater Chem. Phys. 143 (2013) 47e52.
[4] M.H. Al-Saleh, W.H. Saadeh, U. Sundararaj, EMI shielding effectiveness of carbon based nanostructured polymeric materials: a comparative study, Carbon 60 (2013) 146e156.
[5] K. Hu, D.D. Kulkarni, I. Choi, et al., Graphene-polymer nanocomposites for structural and functional applications, Prog. Polym. Sci. 39 (2014) 1934e1972.
[6] S. Cravanzola, S.M. Jain, F. Cesano, et al., Development of a multifunctional TiO2/MWCNT hybrid composite grafted on a stainless steel grating, RSC Adv. 5 (2015) 103255e103264.
[7] E. Fortunati, F. D'Angelo, S. Martino, et al., Carbon nanotubes and silver nanoparticles for multifunctional conductive biopolymer composites, Carbon 49 (2011) 2370e2379.
[8] S. Cravanzola, G. Haznedar, D. Scarano, et al., Carbon-based piezoresistive polymer composites: structure and electrical properties, Carbon 62 (2013) 270e277.
[9] F. Cesano, I. Rattalino, F. Bardelli, et al., Structure and properties of metal-free conductive tracks on polyethylene/multiwalled carbon nanotube composites as obtained by laser stimulated percolation, Carbon 61 (2013) 63e71.
[10] M.J. Uddin, D.E. Daramola, E. Velasquez, et al., A high efficiency 3D photovoltaic microwire with carbon nanotubes (CNT)-quantum dot (QD) hybrid interface, PSS-RRL 8 (2014) 898e903.
[11] M.F.L. De Volder, S.H. Tawfick, R.H. Baughman, et al., Carbon nanotubes: present and future commercial applications, Science 339 (2013) 535e539.
[12] P.M. Ajayan, Nanotubes from carbon, Chem. Rev. 99 (1999) 1787e1800.
[13] V.N. Popov, Carbon nanotubes: properties and application, Mater. Sci. Eng. Rep. 43 (2004) 61e102.
[14] N. Li, Y. Huang, F. Du, et al., Electromagnetic Interference (EMI) shielding of single-walled carbon nanotube epoxy composites, Nano Lett. 6 (2006) 1141e1145.
[15] P. Verma, P. Saini, V. Choudhary, Designing of carbon nanotube/polymer composites using melt recirculation approach: effect of aspect ratio on mechanical, electrical and EMI shielding response, Mater 88 (2015) 269e277.
[16] J. Du, H.-M. Cheng, The fabrication, properties, and uses of graphene/polymer composite, Macromol. Chem. Phys. 213 (2012) 1060e1077.
[17] W. Lin, R. Zhang, C.P. Wong, Modeling of thermal conductivity of graphite nanosheet composites, J. Electron. Mater 39 (2010) 268e272.
[18] S. Pande, A. Chaudhary, D. Patel, et al., Mechanical and electrical properties of multiwall carbon nanotube/polycarbonate composites for electrostatic discharge and electromagnetic interference shielding applications, RSC Adv. 4 (2014) 13839e13849.
[19] P. Verma, P. Saini, R.S. Malik, et al., Excellent electromagnetic interference shielding and mechanical properties of high loading carbonnanotubes/polymer composites designed using melt recirculation equipped twin-screw extruder, Carbon 89 (2015) 308e317.
[20] R. Bell, Conduction in Carbon Nanotube Networks: Large-scale Theoretical Simulations, Springer, Heidelberg, 2015.
[21] S. Iijima, Helical microtubules of graphitic carbon, Nature 354 (1991) 56e58.
[22] Z. Wei, A. Dehghani Sanij, R. Blackburn, Carbon based conductive polymer composites, J. Mater Sci. 42 (2007) 3408e3418.
[23] A.B. Kaiser, V. Skakalova, Electronic conduction in polymers, carbon nanotubes and graphene, Chem. Soc. Rev. 40 (2011) 3786e3801.
[24] R. Sanjines, M.D. Abad, C. Vaju, et al., Electrical properties and applications of carbon based nanocomposite materials: an overview, Surf. Coat. Technol. 206 (2011) 727e733.
[25] D. Stauffer, A. Ahrony, Introduction to the Percolation Theory, Taylor and Francis, London, 1985.
[26] N.G. Sahoo, S. Rana, J.W. Cho, et al., Polymer nanocomposites based on functionalized carbon nanotubes, Prog. Polym. Sci. 35 (2010) 837e867.
[27] I. Alig, P. Pötschke, D. Lellinger, et al., Establishment, morphology and properties of carbon nanotube networks in polymer melts, Polymer 53 (2012) 4e28.
[28] K. Maeda, K. Yamada, K. Yamada, et al., Effect of molecular weight and molecular distribution on skin structure and shear strength distribution near the surface of thin-wall injection molded polypropylene, Open J. Org. Polym. Mater 6 (2016) 1e10.
[29] Z. Li, G. Luo, W. Zhou, et al., Skin-core micro-structure and surface orientation of carbon nanotube composites by injection molding process, Sol. State Phenom. 136 (2008) 51e56.
[30] T. Villmow, S. Pegel, A. John, et al., Liquid sensing: smart polymer/CNT composites, Mater. Today 14 (2011) 340e345.
[31] G. Kasaliwal, A. Göldel, P. Pötschke, Influence of processing conditions in small-scale melt mixing and compression molding on the resistivity and morphology of polycarbonateeMWNT composites, J. Appl. Polym. Sci. 112 (2009) 3494e3509.
[32] P.-C. Ma, N.A. Siddiqui, G. Marom, et al., Dispersion and functionalization of carbon nanotubes for polymer-based nanocomposites: a review, Comp. Part A Appl. Sci. Manuf. 41 (2010) 1345e1367.
[33] S.-J. Park, S.-Y. Lee, F.-L. Jin, Surface modifications of carbon nanotubes for high-performance polymer composites, in: K.K. Kar, J.K. Pandey, S. Rana (Eds.), Handbook of Polymer Nanocomposites Processing, Performance and Application, Springer, Heidelberg, 2015, pp. 13e60.
[34] R.M. Mutiso, K.I. Winey, Electrical properties of polymer nanocomposites containing rod-like nanofillers, Prog. Polym. Sci. 40 (2015) 63e84.
[35] T. Villmow, P. Pötschke, S. Pegel, et al., Influence of twin-screw extrusion conditions on the dispersion of multi-walled carbon nanotubes in a poly(lactic acid) matrix, Polymer 49 (2008) 3500e3509.
[36] M. Monti, I. Armentano, G. Faiella, et al., Toward the microstructureeproperties relationship in MWCNT/epoxy composites: percolation behavior and dielectric spectroscopy, Comp. Sci. Technol. 96 (2014) 38e46.
[37] P.S. Goh, A.F. Ismail, B.C. Ng, Directional alignment of carbon nanotubes in polymer matrices: contemporary approaches and future advances, Comp. Part A Appl. Sci. Manuf. 56 (2014) 103e126.
[38] F. Yu, H. Deng, Q. Zhang, et al., Anisotropic multilayer conductive networks in carbon nanotubes filled polyethylene/polypropylene blends obtained through high speed thin wall injection molding, Polymer 54 (2013) 6425e6436.
[39] D.W. Kang, S.H. Ryu, Orientation of carbon nanotubes in polypropylene melt, Polym. Intern 62 (2013) 152e157.

Relationship between morphology and electrical properties in PP/MWCNT composites: processing-induced anisotropic percolation threshold

F. Cesano*[1], M. Zaccone[2,3] I. Armentano[4], S. Cravanzola[1], L. Muscuso[1], L. Torre[4], J. M. Kenny[3,4] M. Monti[2], and D. Scarano[1]

[1]*Department of Chemistry, NIS (Nanostructured Interfaces and Surfaces) Interdepartmental Centre and INSTM Centro di Riferimento, University of Torino, Via P. Giuria, 7, 10125 Torino, Italy*

[2]*Proplast, Strada Comunale Savonesa 9, 15057 Rivalta Scrivia (AL)*

[3]*ECNP, Strada Comunale Savonesa 9, 15057 Rivalta Scrivia (AL)*

[4]*Università di Perugia, Strada di Pentima 4, UdR INSTM, 05100 Terni (TR)*

Supplementary Data

The DC conductivity of MWCNT/PP composites along the three main directions (X, Y, and Z) was calculated by a scaling law according to the classical percolation threshold theory:

$$\sigma = \sigma_0 (P-P_c)^n$$

for $P>P_c$,

where σ and P are the conductivity (S/cm) and the filler content (wt%) of composites, σ_0 is a scaling factor, and P_c is the percolation threshold.

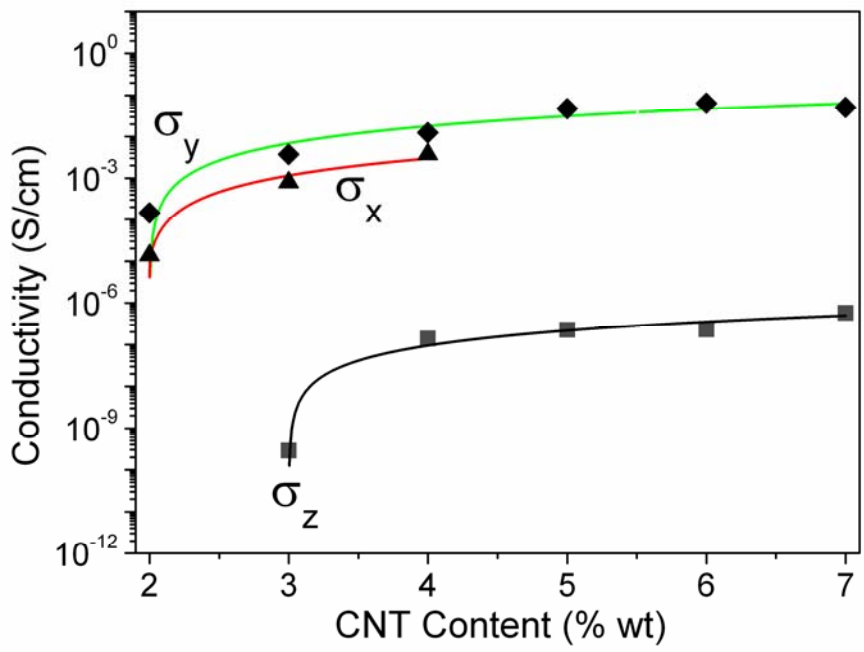

Figure S1. DC conductivity (σ) as a function of MWCNT content for MWCNT/PP composites obtained along the three main directions: σ_x, σ_y and σ_z.

Other references:

D. Stauffer and A., Ahrony, Introduction to the percolation theory, Taylor and Francis, London, 1985;

P. Saini, Intrinsically Conducting Polymer-Based Blends and Composites for Electromagnetic Interference Shielding: Theoretical and Experimental Aspects, ed. P. Saini, John Wiley & Sons, Inc., Hoboken, NJ, USA;

Yang, Y.; Gupta, M. C., Novel Carbon Nanotube−Polystyrene Foam Composites for Electromagnetic Interference Shielding Nano Letters 5, 2005, 2131-2134;

Saini, P., Choudhary, V., Singh, B.P., Mathur, R.B., Dhawan, S.K., Polyaniline-MWCNT nanocomposites for microwave absorption and EMI shielding, Materials Chemistry and Physics 113, 2009, 919-926;